Analysis of Error Coefficients and Improvement of Disturbance Rejection Performance for Active Disturbance Rejection Control System Using the m-*th* order Extended State Observer

YunHak Ri, TaeHyok Kim[1], YongHo Kim
Faculty of Mathematics, **Kim Il Sung** University

ABSTRACT

This paper analyses the disturbance error coefficients for the active disturbance rejection control(ADRC) system and proposes a new method to improve the disturbance rejection performance using the m-*th* order extended state observer(ESO) in order to guarantee the high-precision stabilisation performance of control systems. Using the first order extended state observer in the ADRC system, the disturbance rejection performance is limited due to the disturbance error coefficients. As well, the m-*th* order extended state observer was hardly used for the active disturbance rejection control. In this paper the relationship between error coefficients and gain coefficients of observer and the relationship between error coefficients and natural angular frequency of observer of the ADRC system are analysed for the plant representing in the canonical form according to the extended state order m, and the disturbance rejection performance on the constant, ramp, parabolic and harmonic disturbances is analysed comparing with the results in [32]. The proposed method shows that the constant, ramp and parabolic disturbances are rejected perfectly according to the increase of extended state order m while the rejection performance is improved for the harmonic disturbance of the same frequency by the multiple of m. Taking the merits of principle and method of ADRC and introducing the m-*th* order ESO the disturbance rejection performance can be improved by making the error coefficients to be ‘zero’ according to the extended state order m.

Keywords: active disturbance rejection control, extended state observer, disturbance rejection performance, disturbance error coefficients

[1] The corresponding author. Email: dh.Kim@star-co.net.kp

1. Introduction

Recently it is of great importance to improve the disturbance rejection performance according to the increasing requirements on the tracking precision of control systems [1].

In case that the reference signal and disturbances are measurable or observable, the 2-DOF control would satisfy the requirements of disturbance rejection performance [2]. Robust control and adaptive control are effective for the unstructured internal uncertainties with the bounded parameter variations [3, 4]. The methods to reject the disturbances were proposed by using the internal model principle and estimating the disturbances with observer for the specific structured disturbance model [5]. Recently the ADRC has attracted the interest of control system developers, which is to reject the 'total disturbance'. The ADRC method has the robustness on the parameter uncertainties, total attenuation capability on the external and internal disturbances and the high adaptive capability on the linear and non-linear plants [6, 7]. A method to represent the non-linear control plant in the canonical form with the integral chain structure through some transforms is researched in [7, 8]. Stability was analysed in the frequency-domain for the ADRC on the non-linear time-varying plant with the uncertain dynamic characteristics in [9, 10], and the root locus analysis, describing function method and extended circle criterion were used to analyse the stability of the fast tool servo system in the frequency-domain in [11]. Stability of ADRC systems was researched using non-linear ESO including the fal function or sat function in [14, 15] and most of the other references. Convergence of the (n+1)*th* order ADRC system for the plant with unknown dynamics was proven, and the robustness and the effect of natural angular frequency of observer on the stability and disturbance rejection were analysed in ADRC system with uncertain parameters in [12]. The ESO-based ADRC was studied for the linear system with initial errors in [13], and the position vector control system of PMSM was designed based on the active disturbance rejection controller using the fal function, and the ADRC and velocity compensation controller for the automatic take-off of unmanned aerial vehicles under the various wind conditions were designed in [14, 15]. Missile guidance law using the ADRC was introduced in [15] by focusing on the 3-dimensional guidance in case that the response of autopilot has delays. In [16] the uncertainties in plant and sensors were treated using the adaptive extended state observer(AESO)-based ADRC, and the automatic estimation method was proposed to reduce the estimation error on the state and measuring noise. The ADRC method was studied for MIMO systems in [7, 17]. In [18] the ADRC of high precision servo system was designed to overcome the creeping phenomenon of friction influencing the low velocity performance, and the axis of MEMS gyroscope was driven to resonate and regulate the output amplitude of axis by the ADRC method. [19] showed that selecting the appropriate resonant frequency can reject the sinusoidal disturbances perfectly and implement the ideal reference signal tracking in steady state. The robust absolute stability of the interval non-linear active disturbance rejection-based control system was analysed in [20], and the condition disturbance negation(CDN)-based ADRC was proposed to introduce a method to control the velocity and altitude tracking system of the flexible air-breathing hypersonic flying vehicles in the presence of various uncertainties and disturbances in [21]. The ADRC method was studied to implement the practical output tracking in some non-linear systems in the presence of matched and mismatched uncertainties including the unknown internal systematic dynamic uncertainties, external disturbances and the uncertainties occurred by the difference between control parameters and their nominal values in [22]. The boundary stability of the 1-dimensional instable wave equation influenced by the boundary disturbance was studied in [23], and the ADRC with the actuators saturation characteristics was proposed to reduce the load on the wind turbine drive chain under the condition that the wind speed is slower than the nominal wind speed in [24]. Active control method was proposed to reject the disturbances in the mixed energy source systems used for the mixed electric car in [25], and the enhanced ESO-based control method was proposed to reject the disturbances due to the mismatched uncertainties and external disturbances in the systems without the integral loop in [26]. The fractional-order ADRC method was applied for the precise trajectory tracking and position decision control of the newly designed linear electric motor in [27]. ADRC proposed in [28] has considered the external disturbance and internal uncertainties as total uncertainties, and designed ESO to estimate them in real-time. The practical application is more studied than the theoretical research on the ADRC methods [29-31]. One of the features of ADRC is that it treats the external disturbance and the uncertainties totally in the plant model, and the other one is that it depends rarely on the model and doesn't require the high gain, and it estimates and compensates the real values of the 'total disturbances' using state observer [6, 7]. The fundamentals in the ADRC structure are the canonical form of cascade integrator and the state observer, and its core is ESO [7]. However the cybernetic analysis is not sufficient on the error coefficients in the ADRC system. The differences between extended state variables and the extended state observation variables were evaluated in the most references including [7]. Practically the error of system doesn't reduce even though the difference between the extended state variable and extended state observation variable is very small. The stability and error of control system should meet the required features only by the structure of the system independent of the input signals and disturbances acting on the system in the analysis and design of it. Hence the performance analysis and design of the ADRC system should be done on the basis of structural analysis of the system. However the performance analysis of disturbance rejection of the ADRC was rarely studied based on the analysis of error coefficients. Analysing the error coefficients of ADRC is important in raising the performance of disturbance rejection.

In this paper, the disturbance rejection performance of the ADRC system is analysed with respect to the disturbance error coefficients and the method is studied to improve the disturbance rejection performance.

Firstly, it is shown that the canonical (n+1)*th* order ADRC system becomes the system of the 1st order astatism with respect to the disturbance error while the canonical (n+m)*th* order ADRC system becomes the system of the m-*th* order astatism with respect to the disturbance error.

Secondly, it is shown that the error coefficients are inversely proportional to the 2m-*th* power of the natural angular frequency of observer according to the increase of m in the canonical (n+m)*th* order ADRC system.

Thirdly, it is shown that the harmonic disturbance error is proportional to the m-*th* power of the ratio of the harmonic disturbance frequency to the square of the natural angular frequency of observer when the natural angular frequency of observer is greater than the harmonic disturbance frequency.

The paper consists of the following sections.

Section 2 makes the error model of the (n+m)*th* order ADRC system, and section 3 studies the relationship between the disturbance error coefficients and the gain coefficients of observer for the (n+m)*th* ADRC system. Section 4 analyses the effect of frequency in the (n+m)th linear ADRC system. Section 5 studies the stability of ADRC system using the m-*th* ESO. Section 6 compares and evaluates the errors on the constant, ramp, parabolic and harmonic disturbances according to the extended state order m with the results of [32]. Section 7 provides the corresponding conclusion.

Results show that the disturbance rejection performance is improved greatly in the (n+m)*th* order linear active disturbance rejection control(LADRC) than in the preceding LADRC.

2. Disturbance error model in the (n+m)*th* order active disturbance rejection control system

To consider the problem simply while preserving the generality the model proposed in [7] is adopted.

$$\begin{aligned} &\left.\begin{aligned} &\dot{x}_i(t) = x_{i+1}(t);\ \ (i = \overline{1.n-1}) \\ &\dot{x}_n(t) = F(x_1(t), x_2(t), \cdots x_n(t)) + bu(t) + d(t) \end{aligned}\right\} \ t \geq t_0 \\ &y(t) = x_1(t) \\ &x_i(0) = 0 \end{aligned} \tag{1}$$

Where $X(t)(X(t) = [x_1, x_2, \cdots, x_n]^T \in R^n)$ is the state vector, $y(t)(y(t) \in R)$ is the observable output signal, $u(t)(u(t) \in R)$ is the control input and $u(t)(u(t) \in R)$ is the undefined non-linear function. Here the disturbance error coefficients are discussed in the problem where output signal $y(t)$ tracks the reference signal $r(t)$.

Assumption 1. The nominal value of b is b_0, and b is uncertain parameter satisfying $b > 0,\ \ b \in [b_{\min}, b_{\max}]$.

Assumption 2. Eq.(1) is represented as the canonical form of the linear chain of integrators from [7].

Assumption 3. m is the extended order of system.

Assumption 4. Eq.(1) is controllable by the feedback control.

Assumption 5. External disturbance $d(t)$ is introduced from [19] and can be considered to the extended order as follows.

$$\begin{aligned} d(t) &= d_1(t) + d_2(t) \\ d_1 &= \sum_{i=1}^{m} \alpha_{i-1} t^{i-1}; \quad |d_1(t)| \le \bar{d}_1; \\ d_2 &= A \sin \omega_d t; \quad |d_2(t)| \le \bar{d}_2 \end{aligned} \tag{2}$$

Where $d_1(t)$ is aperiodic disturbance, α_{i-1} is maximum of derivative of $d_1(t)$, the m-*th* order derivative of $d_1(t)$ is zero.

$d_2(t)$ is harmonic disturbance, and $A(|A| \le \bar{A})$ and $\omega_d(\omega_d \le \bar{\omega}_d)$ are amplitude and angular frequency of $d_2(t)$. α_{i-1}, A and ω_d are uncertain quantities.

Assumption 6. In Eq.(1) considering the Assumption 1 and Assumption 2, lump disturbance

$$w(F,d,b,t) = F(x_1(t), x_2(t), \cdots x_n(t)) + d(t) + (b(t) - b_0)u \tag{3}$$

reflecting the internal uncertainties and external disturbances satisfies Lipschitz condition.

Assumption 7. To analyse the error coefficients and evaluate the disturbance rejection performance for the active disturbance rejection control system, the reference signal is assumed as follows: $r(t) = 0$

From Eqs.(3) and (1) can be written as

$$\begin{aligned} &\left.\begin{aligned} \dot{x}_i(t) &= x_{i+1}(t); \ (i = \overline{1.n-1}) \\ \dot{x}_n(t) &= w(F,d,b,t) + b_0 u(t) \end{aligned}\right\} t \ge t_0 \\ &y(t) = x_1(t) \\ &x_i(0) = 0 \end{aligned} \tag{4}$$

In Eq.(4), denoting the extended state variable $x_{n+1}(t)$ as

$$x_{n+1}(t) = w(F,b,d,t) = h(t) \tag{5}$$

and differentiating Eq.(5) m times, and then substituting into Eq.(4), it can be represented as the canonical m-*th* order extended state model.

$$\begin{aligned} &\left.\begin{aligned} \dot{x}_i(t) &= x_{i+1}(t); i = \overline{1, n-1} \\ \dot{x}_n(t) &= x_{n+1}(t) + b_0 u; \\ \dot{x}_{n+j}(t) &= x_{n+j+1}(t); \quad j = \overline{1, m-1}; \\ \dot{x}_{n+m}(t) &= h^{(m)}(t) \end{aligned}\right\} \\ &y(t) = x_1(t) \end{aligned} \tag{6}$$

Where m is the extended state order and $h^{(m)}$ is the m-*th* order derivative of $h(t)$.
The m-*th* order extended state observer on Eq.(6) can be represented as

$$\left.\begin{array}{l}\dot{\hat{x}}_i(t)=\hat{x}_{i+1}(t)+\beta_i(y(t)-\hat{y}(t));\ (i=\overline{1.n-1})\\ \dot{\hat{x}}_n(t)=\hat{x}_{n+1}(t)+b_0u(t)+\beta_n(y(t)-\hat{y}(t))\\ \dot{\hat{x}}_{n+j}(t)=\hat{x}_{n+j+1}(t)+\beta_{n+j}(y(t)-\hat{y}(t));\ (j=\overline{1,m-1})\\ \dot{\hat{x}}_{n+m}(t)=\beta_{n+m}(y(t)-\hat{y}(t))\end{array}\right\}\ t\geq t_0 \tag{7}$$
$$\hat{y}(t)=\hat{x}_1(t)$$

Where $\hat{x}_i(t)$ is the state vector of observer, $\hat{y}(t)$ is the output signal of observer and β_i is the gain coefficients of observer whose characteristic polynomial $s^{n+m}+\sum_{i=1}^{n+m}\beta_i s^{n+m-i}$ satisfies the Hurwitz criterion. If the disturbance on the control plant can be observed from the ESO the control law is represented as

$$u(t)=-\frac{\hat{x}_{n+1}(t)}{b_0}+u_{ref}(t) \tag{8}$$

Where $\hat{x}_{n+1}(t)$ is the observation value of $x_{n+1}(t)$.
In Eq.(8), let's denote the control law u_{ref} as follows.

$$u_{ref}(t)=-\sum_{i=1}^{n}f_ie_i \tag{9}$$

Where f_i is the state feedback coefficient, and $e_i(t)=r_i(t)-x_i(t)$ is the i-*th* state error of the system. Considering the Assumption 7, Eq.(9) is represented as follows.

$$u_{ref}(t)=\sum_{i=1}^{n}f_ix_i \tag{10}$$

Considering Eq.(10) in Eq.(8), it is denoted as follows.

$$u(t)=-\frac{\hat{x}_{n+1}(t)}{b_0}-\sum_{i=1}^{n}f_ix_i(t) \tag{11}$$

Substituting Eq.(11) into Eq.(4),

$$\left.\begin{array}{l}\dot{x}_i(t)=x_{i+1}(t);\ (i=\overline{1.n-1})\\ \dot{x}_n(t)=w(F,d,b,t)-\hat{x}_{n+1}(t)-b_0f_ix_i(t)\end{array}\right\}t\geq t_0 \tag{12}$$
$$y(t)=x_1(t),\quad x_i(0)=0$$

Substituting Eq.(11) into Eq.(7),

$$\left.\begin{aligned}
&\dot{\hat{x}}_i(t)=\hat{x}_{i+1}(t)+\beta_i(y(t)-\hat{y}(t));\ \ (i=\overline{1.n-1})\\
&\dot{\hat{x}}_n(t)=\beta_n(y(t)-\hat{y}(t))-b_0 f_i x_i(t)\\
&\dot{\hat{x}}_{n+j}(t)=\hat{x}_{n+j+1}(t)+\beta_{n+j}(y(t)-\hat{y}(t));\ \ (j=\overline{1,m-1})\\
&\dot{\hat{x}}_{n+m}(t)=\beta_{n+m}(y(t)-\hat{y}(t))
\end{aligned}\right\}\ t\geq t_0 \tag{13}$$

$$\hat{y}(t)=\hat{x}_1(t)$$

Using Laplace transformation of Eq.(12), $E(s)$ can be found as

$$E(s)=\frac{\hat{X}_{n+1}(s)-W(s)}{\left(s^n+b_0\sum_{i=1}^{n} f_i\ s^{i-1}\right)} \tag{14}$$

Where $E(s),W(s)$ and $\hat{X}_{n+1}$ are the Laplace transformations of $e(t),w(t)$ and $\hat{x}_{n+1}$.

Let's represent the observer error as

$$\hat{e}(t)=y(t)-\hat{y}(t)=r(t)-e(t)-\hat{y}(t) \tag{15}$$

Using the Laplace transformations of Eqs.(13) and (15) the observer error can be written as

$$\hat{E}(s)=\frac{-(s^n+b_0\sum_{i=1}^{n} f_i s^{i-1})E(s)}{s^n+\sum_{i=1}^{n}\beta_i s^{n-i}} \tag{16}$$

On one hand, from the Laplace transformation of the (n+1)*th* order term to the (n+m)*th* order term for Eq.(13), the extended state value $\hat{X}_{n+1}(s)$ can be found as

$$\hat{X}_{n+1}(s)=\frac{\left(\sum_{j=1}^{m}\ \beta_{n+j}s^{m-j}\right)}{s^m}\hat{E}(s) \tag{17}$$

Substituting Eq.(16) into Eq.(17),

$$\hat{X}_{n+1}(s)=\frac{-(s^n+b_0\sum_{i=1}^{n} f_i s^{i-1})E(s)}{s^m(s^n+\sum_{i=1}^{n}\beta_i s^{n-i})} \tag{18}$$

On the other hand, substituting Eq.(18) into Eq.(14) the error model of LADRC system can be found as follows using the m-*th* order extended state observer.

$$E(s)=\frac{-s^{m}\cdot\left(s^{n}+\sum_{i=1}^{n}\beta_{i}s^{n-i}\right)W(s)}{s^{m}\left(s^{n}+\sum_{i=1}^{n}\beta_{i}s^{n-i}\right)\left(s^{n}+b_{0}\sum_{i=1}^{n}f_{i}s^{i-1}\right)+\left(\sum_{j=1}^{m}\beta_{n+j}s^{m-j}\right)\left(s^{n}+b_{0}\sum_{i=1}^{n}f_{i}s^{i-1}\right)} \tag{19}$$

3. Analysis of disturbance error coefficients in the (n+m)*th* order linear active disturbance rejection control system

From Eq.(19) the error transfer function from the lump disturbance to the error is as follows.

$$\Phi_{w-e}(s)=\frac{s^{m}\cdot\left(s^{n}+\sum_{i=1}^{n}\beta_{i}s^{n-i}\right)W(s)}{s^{m}\left(s^{n}+\sum_{i=1}^{n}\beta_{i}s^{n-i}\right)\left(s^{n}+b_{0}\sum_{i=1}^{n}f_{i}s^{i-1}\right)+\left(\sum_{j=1}^{m}\beta_{n+j}s^{m-j}\right)\left(s^{n}+b_{0}\sum_{i=1}^{n}f_{i}s^{i-1}\right)} \tag{20}$$

Where $\Phi_{w-e}(s)$ is the error transfer function on the disturbance.

The error coefficients in Eq.(20) are represented as follows.

$$C_{i}=\frac{\partial}{\partial s}\Phi_{w-e}(s)_{S=0};\ i=\overline{0,m} \tag{21}$$

Where C_i is the error coefficients and $\Phi_{w-e}(\mathrm{s})$ is the transfer function from disturbance to error.

The following results can be found from Eq.(21).

Remark 1. The canonical (n+1)*th* order ADRC system becomes the system of the 1st order astatism with respect to the disturbance error when $m=1$, and the system can't make the disturbance error to be 'zero' on the other disturbances besides the constant disturbance theoretically. Let's analyse the disturbance error coefficients for several systems.

1) For $n=3,\ m=1$

The disturbance error transfer function of ADRC system from Eq.(20) is as follows.

$$\Phi_{d-e}(s)=\frac{(s^{4}+C_{3}s^{3}+C_{2}s^{2}+C_{1}s)}{s^{7}+A_{6}s^{6}+A_{5}s^{5}+A_{4}s^{4}+A_{3}s^{3}+A_{2}s^{2}+A_{1}s+A_{0}} \tag{22}$$

Where

$$A_{6}=\beta_{1}+b_{0}f_{3},$$
$$A_{5}=\beta_{2}+\beta_{1}b_{0}f_{3}+b_{0}f_{2},$$

$$A_4 = \beta_3 + \beta_2 b_0 f_3 + \beta_1 b_0 f_2 + b_0 f_1,$$
$$A_3 = \beta_4 + \beta_3 b_0 f_3 + \beta_2 b_0 f_2 + \beta_1 b_0 f_1,$$
$$A_2 = \beta_4 b_0 f_3 + \beta_3 b_0 f_2 + \beta_2 b_0 f_1,$$
$$A_1 = \beta_4 b_0 f_2 + \beta_3 b_0 f_1,$$
$$A_0 = b_0 f_1 \beta_4,$$
$$C_4 = 1,\ C_3 = \beta_1,\ C_2 = \beta_2,\ C_1 = \beta_3,$$

2) For $n = 2,\ m = 1$

The disturbance error transfer function of ADRC system from Eq.(20) is as follows.

$$\Phi_{d-e}(s) = \frac{(C_3 s^3 + C_2 s^2 + C_1 s)}{s^5 + A_4 s^4 + A_3 s^3 + A_2 s^2 + A_1 s + A_0} \tag{23}$$

Where

$$A_4 = \beta_1 + b_0 f_2,$$
$$A_3 = \beta_2 + \beta_1 b_0 f_2 + b_0 f_1,$$
$$A_2 = \beta_3 + \beta_2 b_0 f_2 + \beta_1 b_0 f_1,$$
$$A_1 = \beta_3 b_0 f_2 + \beta_2 b_0 f_1,$$
$$A_0 = \beta_3 b_0 f_1,$$
$$C_3 = 1, \qquad C_2 = \beta_1, \qquad C_1 = \beta_2$$

3) For $n = 1,\ m = 1$

The disturbance error transfer function of ADRC system from Eq.(20) is

$$\Phi_{d-e}(s) = \frac{(C_2 s^2 + C_1 s)}{s^3 + A_2 s^2 + A_1 s + A_0} \tag{24}$$

Where

$$A_2 = \beta_1 + b_0 f_1, \quad A_1 = \beta_2 + b_0 f_1 \beta_1, \quad A_0 = b_0 f_1 \beta_2$$

$$C_2 = 1, \quad C_1 = \beta_1$$

From Eqs.(22)-(24) the disturbance error coefficients using Eq.(21) can be found as in table 1.

table1. Error coefficients according to the plant order in LADRC

Error Coefficients \ Plant order	$n=1,\ m=1$	$n=2,\ m=1$	$n=3,\ m=1$
C_{0d}	0	0	0
C_{1d}	$\frac{\beta_1}{f_1\beta_2}$,	$\frac{\beta_2}{f_1\beta_3}$,	$\frac{\beta_3}{f_1\beta_4}$,
C_{2d}	$\neq 0$	$\neq 0$	$\neq 0$

Remark 2. Canonical (n+m)*th* order LADRC system becomes the system of astatism of the m-*th* order with respect to the disturbance according to the extended state order m.

1) For $n=1, m=1$

From Eq.(20) the disturbance error transfer function of system is same as Eq.(24).

2) For $n=1, m=2$

From Eq.(20) the disturbance error transfer function of system is represented as

$$\Phi_{d-e}(s) = \frac{(C_3 s^3 + C_2 s^2)}{s^4 + A_3 s^3 + A_2 s^2 + A_1 s + A_0} \tag{25}$$

Where

$$\begin{aligned}
A_3 &= \beta_1 + b_0 f_1, \\
A_2 &= \beta_2 + b_0 f_1 \beta_1, \\
A_1 &= \beta_3 + b_0 f_1 \beta_2, \\
A_0 &= b_0 f_1 \beta_3, \\
C_3 &= 1, \qquad C_2 = \beta_1,
\end{aligned}$$

3) For $n=1, m=3$

From Eq.(20) the disturbance error model of system is as follows.

$$\Phi_{d-e}(s) = \frac{(C_4 s^4 + C_3 s^3)}{s^5 + A_4 s^4 + A_3 s^3 + A_2 s^2 + A_1 s + A_0} \tag{26}$$

where

$$\begin{aligned}
A_4 &= \beta_1 + b f_1, \\
A_3 &= \beta_2 + b f_1 \beta_1, \\
A_2 &= \beta_3 + b f_1 \beta_2, \\
A_1 &= \beta_4 + b f_1 \beta_3, \\
A_0 &= b f_1 \beta_4, \\
C_4 &= 1, \quad C_3 = \beta_1,
\end{aligned}$$

From Eqs.(24)-(26) the disturbance error coefficients using Eq.(21) can be found as in table 2.

table 2**.** Error coefficients according to the extended state order m in LADRC

Error Coefficients \ Plant	$n=1, m=1$	$n=1, m=2$	$n=1, m=3$
C_{0d}	0	0	0
C_{1d}	$\frac{\beta_1}{f_1 \beta_2}$,	0	0
C_{2d}	$\neq 0$	$\frac{2\beta_1}{f_1 \beta_3}$	0
C_{3d}	$\neq 0$	$\neq 0$	$\frac{3\beta_1}{f_1 \beta_4}$

Corollary. Canonical (n+m)*th* order ADRC system can make the disturbance errors up to the m-*th* order to be ‘zero’ theoretically.

4. Analysis of frequency effect in the (n+m)*th* order LADRC system

4.1. Analysis of Effect of Natural Angular Frequency in the (n+m)th Order LADRC System.

Remark 3. Error coefficients of the canonical (n+m)*th* order LADRC system are inversely proportional to the 2m-*th* power of the natural angular frequency of observer.

To explain the Remark 3 the error dynamics of the system can be found from Eqs.(6) and (7) as follows.

$$\left.\begin{aligned}&\dot{x}_{e\,i}(t) = x_{e_i(i+1)}(t) - \beta_i x_{e1}(t);\ \ (i = \overline{1.n-1}),\\ &\dot{x}_{e\,n}(t) = \hat{x}_{e\ (n+1)}(t) - \beta_n x_{e1}(t)\\ &\dot{x}_{e(n+j)}(t) = x_{e(n+j+1)}(t) - \beta_{n+j} x_{e1}(t);\ \ j = \overline{1,m-1};\\ &\dot{x}_{e(n+m)}(t) = h^{(m)}(t)\end{aligned}\right\} \quad (27)$$

$$\hat{e}(t) = x_{e1}(t)$$

Where $x_{e\,i}(t)(x_{e\,i}(t) = x_i(t) + \hat{x}_i(t))$ is the error state variable of observer.

The characteristic equation of Eq.(27) is expressed as

$$D_C(s) = s^{n+m} + \sum_{i=1}^{n+m} \beta_i s^{n+m-i} \quad (28)$$

Where $D_C(s)$ is the characteristic equation of observer.

From the Hurwitz criterion characteristic polynomial

$$D_{0C}(s) = (s + \omega_C)^{n+m} \quad (29)$$

the gain coefficients of observer can be written as

$$\beta_i = \alpha_i \omega_C^i \quad (30)$$

Where α_i is binomial coefficient and ω_C is the natural angular frequency of observer.

The characteristic equation of Eq.(12) can be written as

$$D(s) = s^n + b_0 \sum_{i=1}^{n} f_i\ s^{i-1} \quad (31)$$

From Hurwitz criterion characteristic polynomial

$$D_0(s) = (s + \omega_0)^n \quad (32)$$

the coefficients of controller can be written as

$$f_i = \mu_i \omega_0^i \quad (33)$$

Where μ_i is the binomial coefficient and ω_0 is the natural angular frequency of controller.

Let’s set the relationship between the natural angular frequencies of controller and observer as

$$\omega_C = k_C \omega_0 \quad (34)$$

Where k_C is a scale factor and given by the designer.

Applying the results of Eqs.(30), (33) and (34) to table 2 gives the following table.

table 3. Error coefficients according to the natural angular frequency in the (n+m)*th* order LADRC

Plant / Error Coefficients	$m=1$	$m=2$	$m=3$
C_{0d}	0	0	0
C_{1d}	$\frac{2k_C}{\omega_C^2}$,	0	0
C_{2d}	$\neq 0$	$\frac{6k_C^2}{\omega_C^4}$	0
C_{3d}	$\neq 0$	$\neq 0$	$\frac{12k_C}{\omega_C^6}$

4.2. Analysis of the Harmonic Disturbance Rejection Performance in the (n+m)th Order LADRC System.

Remark 4. The maximum value of error on the harmonic disturbance is proportional to $\left(k_C \frac{\overline{\omega}_d}{\omega_C^2}\right)^m$ for $\overline{\omega}_d < \omega_C$ in the canonical (n+m)*th* order LADRC system.

From Assumption 2 and Eq.(2), the maximum value of the harmonic disturbance according to m is written as

$$d_{2i\_\max} = |A||\omega_d|^{(i-1)} \tag{35}$$

Where $i(i=\overline{1,m})$ is the order of the derivative on the disturbance d_2.

From Eqs.(35) and (21) the maximum value of error on the disturbance d_2 can be written as

$$|e_{d2-e}|_{\max} = \sum_{i=1}^{m} C_i d_{2i\_\max} = \sum_{i=1}^{m} C_i(\omega_0, \omega_C)|A||\omega_d|^{(i-1)} \tag{36}$$

From Table 3 and Eq.(36) the maximum harmonic disturbance error according to the increase of m is illustrated in table 4.

table 4. Maximum value of the harmonic disturbance error according to the order m

m	$m=1$	$m=2$	$m=3$
$\lvert e_{d-e}\rvert_{\max}$	$2\lvert A\rvert\left(k_C \frac{\overline{\omega}_d}{\omega_C^2}\right)$	$6\lvert A\rvert\left(k_C \frac{\overline{\omega}_d}{\omega_C^2}\right)^2$	$12\lvert A\rvert\left(k_C \frac{\overline{\omega}_d}{\omega_C^2}\right)^3$

5. Stability of LADRC system using the m-*th* order ESO

The dynamics of ADRC system depends on $F(x_1, x_2, \cdots, x_n, t)$, where the m-*th* order ESO is combined with the plant with unknown dynamics.

Combining Eqs.(12) and (13) into simultaneous equations

$$\left.\begin{array}{l} \dot{X}(t) = AX(t) + B_{WW} w(t) \\ y = CX(t) \end{array}\right\} \tag{37}$$

Where

$$X(t) = [X_N, \hat{X}_{N+M}]^T \in R^{n \times m},$$

$$X_N(t) = [x_1, x_2, \cdots, x_n]^T \in R^{n \times 1},$$

$$\hat{X}_N(t) = [\hat{x}_1, \hat{x}_2, \cdots, \hat{x}_n]^T \in R^{n \times 1},$$

$$\hat{X}_M(t) = [\hat{x}_{n+1}, \hat{x}_{n+2}, \cdots, \hat{x}_m]^T \in R^{m \times 1},$$

$$A = \begin{bmatrix} A_N - B_N F_N & 0_{(n \times n)} & B_N F_M \\ -\beta_N C_N & A_N - B_N F_N - \beta_N C_N & 0_{(m \times m)} \\ -\beta_M C_M & 0_{(n \times n)} & A_M \end{bmatrix} \in R^{(n+m) \times (n+m)},$$

$$B_{WW} = \begin{bmatrix} B_W \\ 0 \\ 0 \end{bmatrix} \in R^{(n+m) \times 1},$$

$$C = \begin{bmatrix} C_N & 0 \end{bmatrix} \in R^{(n+m) \times 1},$$

$$A_N = \begin{bmatrix} 0 & 1 & \cdots & 0 \\ \cdots & \cdots & \cdots & \cdots \\ 0 & 0 & \cdots & 1 \\ 0 & 0 & \cdots & 0 \end{bmatrix} \in R^{n \times n},$$

$$B_N = \begin{bmatrix} 0 \\ \cdots \\ 0 \\ b_0 \end{bmatrix} \in R^{n \times 1},$$

$$F_N = \begin{bmatrix} f_1 & f_2 & \cdots & f_n \end{bmatrix} \in R^{1 \times n},$$

$$B_W = \begin{bmatrix} 0 \\ \cdots \\ 0 \\ 1 \end{bmatrix} \in R^{n \times 1},$$

$$A_M = \begin{bmatrix} 0 & 1 & \cdots & 0 \\ \cdots & \cdots & \cdots & \cdots \\ 0 & 0 & \cdots & 1 \\ 0 & 0 & \cdots & 0 \end{bmatrix} \in R^{m \times m},$$

$$\beta_N = \begin{bmatrix} \beta_1 \\ \cdots \\ \beta_n \end{bmatrix} \in R^{n \times 1},$$

$$\beta_M = \begin{bmatrix} \beta_{n+1} \\ \cdots \\ \beta_m \end{bmatrix} \in R^{m \times 1},$$

$$F_M = \begin{bmatrix} -1 & 0_{m \times m-1} \end{bmatrix} \in R^{m \times m},$$

System of Eq.(37) will be stable provided that the gain coefficients $f_i = \mu_i \omega_0^i$ of controller satisfying Eqs.(30)~(33) for $w(t) = 0$ and the gain coefficients $\beta_i = \alpha_i \omega_C^i$ of observer are determined. For $w(t) \neq 0$ the proof on the stability can be referred from [7, 12, 32] if $w(t)$ satisfies the Lipschitz condition.

6. Simulation results

6.1 Simulation on the Disturbance Error Feature according to the Extended Order.

For simulation and analysis the model of the control plant is given as

$$\left.\begin{aligned} \dot{x} &= u + d \\ y &= x \end{aligned}\right\} \tag{38}$$

Disturbance d contains the constant, ramp, parabolic and harmonic disturbances from Eq.(2).

$$\begin{aligned} d &= f_P + f_S \\ f_P &= f_0 + f_1 t + f_2 t^2 + f_{m-1} t^{(m-1)} \\ f_S &= A\sin(\omega_r t) \end{aligned} \tag{39}$$

For $x_2 = d$ and $m = 3$, the m-*th* order extended state model is as follows.

$$\left.\begin{aligned} \dot{x}_1 &= u + x_2 \\ \dot{x}_{1+j} &= x_{1+j+1} \ ; \quad j = \overline{1, m-1} \\ x_{1+m} &= d^{(m)} \\ y &= x_1 \end{aligned}\right\} \tag{40}$$

The ESO is as follows.

$$\left.\begin{aligned} \dot{\hat{x}}_1 &= u + \hat{x}_2 + \beta_1 (y - \hat{y}) \\ \dot{\hat{x}}_{1+j} &= \hat{x}_{1+j+1} - \beta_{1+j} (y - \hat{y}); \quad j = \overline{1, m-1} \\ \dot{\hat{x}}_{1+m} &= \beta_{1+m} (y - \hat{y}) \\ \hat{y} &= \hat{x}_1 \end{aligned}\right\} \tag{41}$$

The ADRC law and control law of regulator are designed by the proposed design method and can be written as

$$\left.\begin{aligned} u &= -x_2 + u_0 \\ u_0 &= k_1 (r - y) + k_2 \dot{r} \end{aligned}\right\} \tag{42}$$

Where $r=0$ is reference signal, and k_1 and k_2 are the transfer coefficients of controller, and $k_1=100$, $k_2=1$.

Values of β_i according to the extended state order are given in table 5.

table 5. β_i according to the extended state order and the angular velocity.

m	Values of β_i for $\omega_C=30\ 1/s$				
	β_1	β_2	β_3	β_4	
1	$2\cdot 30$	30^2			
2	$3\cdot 30$	$3\cdot 30^2$	30^3		
3	$4\cdot 30$	$6\cdot 30^2$	$4\cdot 30^3$	30^4	
4	$5\cdot 30$	$10\cdot 30^2$	$10\cdot 30^3$	$5\cdot 30^4$	30^5

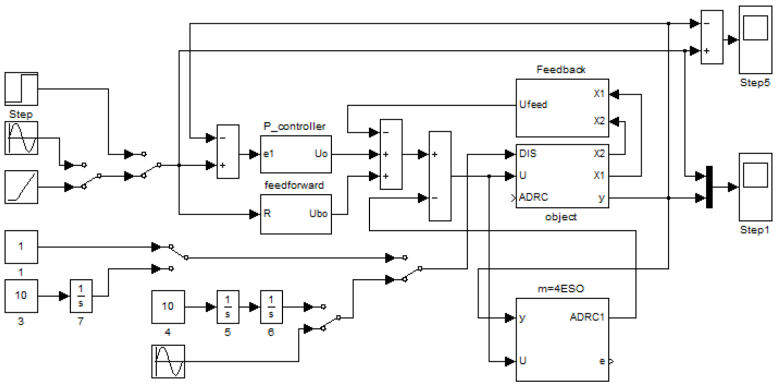

Figure1. Block diagram of the system designed by the proposed method.

The transient and tracking features of the system are as follows.

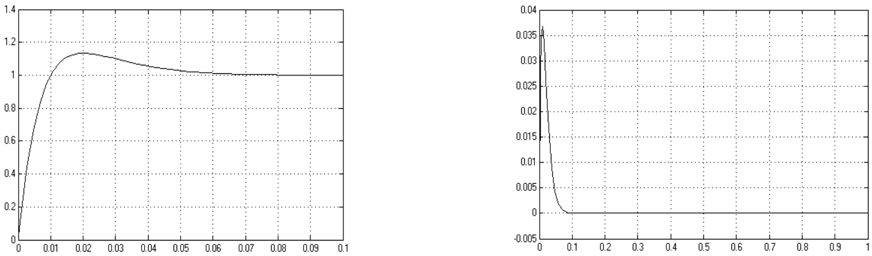

Figure 2. Features of the proposed system(transient feature on left, velocity tracking feature on the right)

In Eq.(39) the simulation conditions on the disturbances are $f_0=1$, $f_1=10\ 1/\mathrm{s}$, $f_2=10\ 1/\mathrm{s}^2$, $A=1$, $\omega_d=10\ 1/\mathrm{s}$.

(1) Constant disturbance rejection feature according to m

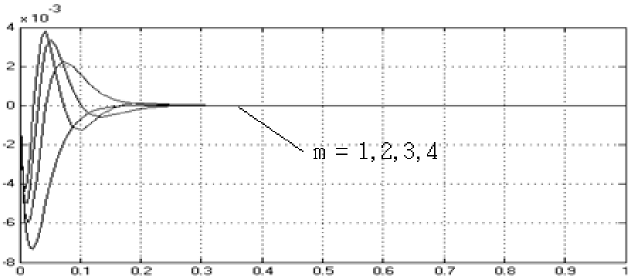

Figure 3. Constant disturbance rejection feature according to m .

Fig 3 shows ESO is astatic on the disturbances.

(2) Constant ramp disturbance rejection feature according to m

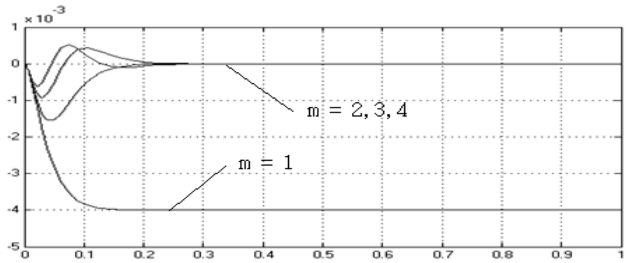

Figure 4. Constant ramp disturbance rejection feature according to m .

Fig 4 shows the 1st order ESO is 1st order astatic on the disturbances.

(3) Constant parabolic disturbance rejection feature according to m

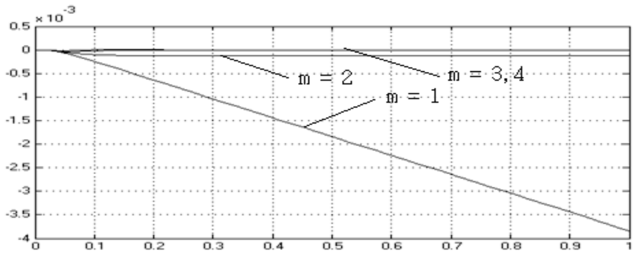

Figure 5. Constant parabolic disturbance rejection feature according to m .

Fig 5 shows the 2nd order ESO is 2nd order astatic on the disturbances.

(4) Harmonic disturbance rejection feature according to m

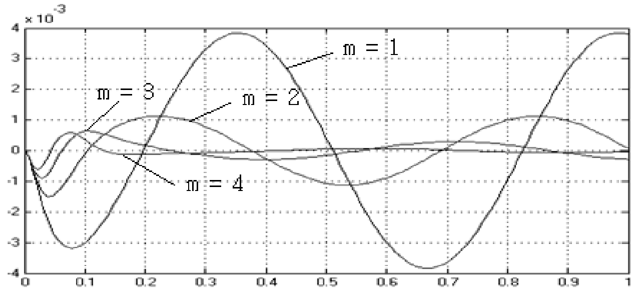

Figure 6. Harmonic disturbance rejection feature according to m .

Fig 6 shows the harmonic disturbance rejection performance of the m-*th* order ESO is getting better according to the increase of m .

6.2 Comparison of the Proposed Design Method with the Preceding ADRC System.

The design and simulation data in [32] are used to compare and evaluate the feature of the proposed design method.

The system model in [32] is as follows.

$$\left.\begin{aligned} &\dot{x}_1(t) = x_2(t) \\ &\dot{x}_2(t) = -a_1 x_1(t) + a_2 x_2(t) + bu + d(t) \end{aligned}\right\} \\ y(t) = x_1(t) \\ x_1(0) = 0, \;\; x_2(0) = 0, \;\; y(0) = 0 \tag{43}$$

Where $|d(t)| \le 1,\ |d(t)| \le 0.5,\ |a_i| \le 2;\ i = 1,2,\ b/b_0 \in [0.5,3],\ b_0 = 1$.

For $e(t) = r(t) - y(t)$, the controller can be written as

$$u(t) = -\tilde{e}_3 - k_1 \tilde{e}_2 - k_2 \tilde{e}_1 \tag{44}$$

The controller parameters are $k_1 = 4$ and $k_2 = 4$.

From [32] the parameter uncertainty and disturbance conditions are given in table 6.

table 6. Parameter uncertainties and disturbances for comparison.

No	Item	a_1	a_2	b	ω_C	$d(t)$
1	$C1-1$	-0.1	2	0.5	30	$\sin(0.08\pi\ t)$
2	$C2-2$	0.6	-0.8	1.3	30	$\sin(0.1\pi\ t)$
3	$C3-4$	-1.6	-0.5	2.1	30	1

The (n+m)*th* order ADRC system can be designed for the (43) are compared with the (n+1)*th* order and (n+2)*th* order ADRC as follows.

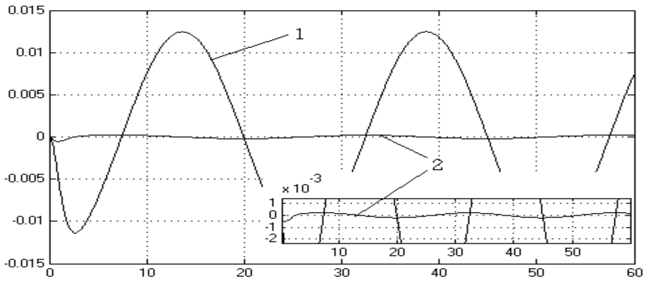

Figure 7. Feature comparison for $C1-1$(1-for n+1, 2-for n+2).

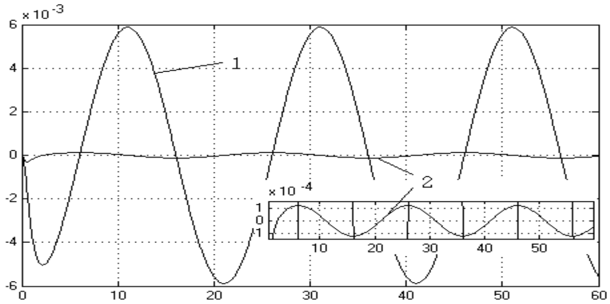

Figure 8. Feature comparison for $C2-2$.(1-for n+1, 2-for n+2).

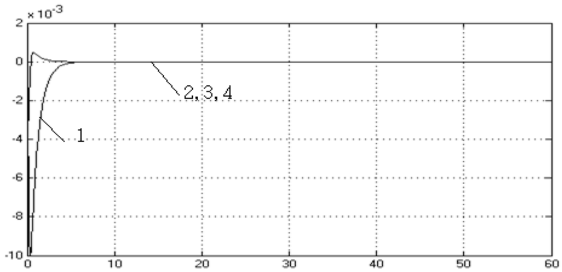

Figure 9. Feature comparison for $C3-4$.

Comparing with the results in [32] the disturbance rejection performance for $m=2$ is given in table 7.

table 7. Comparison with [32] for $m=2$.

Item	$C1-1$	$C2-2$	$C3-4$
Ratio of Disturbance Rejection	34.7 times	58.82 times	-

Fig 7 and Fig 8 show that the disturbance rejection performance has been improved further for $m=2$ than for $m=1$.

Fig 9 shows that uncertainties independent of time change and the constant disturbances can be removed totally by the active disturbance rejection performance.

7. Conclusion

In this paper, the error coefficients of the ADRC system were analysed using the m-*th* order ESO to guarantee the high-precision tracking performance of the control system and a method is proposed to improve the disturbance rejection performance. Corresponding analysis has evaluated the relationship between the error coefficients and the gain coefficients of observer, the relationship between the error coefficients and the natural angular frequency of observer and the relationship between the error coefficients and the frequency of harmonic disturbance. Results show that the proposed method has overcome the limitation of the first order ESO that the disturbance rejection depends only on the increase of natural angular frequency of observer by using the m-*th* order ESO and the disturbance rejection performance can be raised by changing the natural angular frequency of observer and the error coefficients simultaneously according to m. The disturbance rejection capability of the system using the m-*th* order ESO has been confirmed through the simulation and comparison. It has been verified that using the m-*th* order ESO is an advanced method to raise the disturbance rejection capability of the system in the ADRC system.

References

[1] Basar T. Contol theory: twenty-five seminal papers. New York: IEEE press 2001.

[2] Yang K, Choi Y, Chung W K, Sun I H, Oh S R. On the tracking performance Improvement of Optical Disk Drive Servo System Using Error-Based Disturbance Observer. IEEE Tran, Industronics 2005; 52: 270-280.

[3] Feng G, Liu Y, Huang L. A new robust algorithm to improve the dynamic performance on the speed control of induction motor drive. IEEE. Trans Power Electron 2004; 19: 1624-7.

[4] Chu L, Yi H H. Adaptive feedforward control for disturbance torque rejection in seeker stabilizing loop. IEEE Trans control syst tech 2011; 9.

[5] Kwon S, Chung W K. A discrete-time design and analysis of perturbation observer for motion control application. IEEE Trans Control System Technol. 2003; 11: 399-407.

[6] Han J. Active disturbance rejection controller and its applications. Control. Decis 1998; 13: 19-23.

[7] Huang Y, Xue W C. Active disturbance rejection control: Methodology and theoretical analysis. ISA Transactions 2014; 53: 963-976.

[8] Zhang C L, Yang J, Li S H. Homogeneous Active Disturbance Attenuation for a Perturbed Chain of Integrators. IFAC-Papers On Line 2016; 49: 534-539.

[9] Guo B Z, Wu Z H, Zhou H C. Active disturbance rejection control approach to output-feedback stabilization of a class of uncertain nonlinear system subject to

stochastic disturbance. IEEE Trans on Automatic control 2015; 2471815.

[10] Zheng Q, Chen Z, Gao Z. A practical approach to disturbance decoupling control. Eng Pract 2014;17: 1016-25.

[11] Li J, Qi X H, Xia Y Q, Pu F, Chang K. Frequency domain stability analysis of nonlinear active disturbance rejection control system. ISA Transactions Journal homepage: www.elsevier.com/locate/ isatrans 2010.

[12] Talole S E, Kolhe J P, Phadke S B. Extended-state-observer-based control of flexible-joint system with experimental validation. IEEE Trans Ind Electron 2010; 57: 1411-9.

[13] Hua X X, Huang D R, Guo S H. Extended State Observer Based on ADRC of Linear System with Incipient Fault. International Journal of Control, Automation and System 2020; 18: 1-10.

[14] Gao B W, Shao J P, Yang X D. A compound control strategy combining velocity compensation with ADRC of electro-hydraulic position servo control system. ISA Transactions 2014; 53: 1910-1918.

[15] Yuan Y B, Zhang K. Design of robust guidance law via active disturbance rejection control. Journal of Systems Engineering and Electronics 2015; 26: 353-358.

[16] Xue W C. ADRC with Adaptive Extended State Observer and its Application to Air-Fuel Ratio Control in Gasoline Engines. IEEE Transactions on Industrial Electronics 2015; 62.

[17] Xue W, Huang Y. On performance analysis of ADRC for a class of MIMO lower-triangular nonlinear uncertain system. ISA Tran 2014; 53: 955-62.

[18] Zheng Q, Dong L L, Lee D H, Gao Z Q. Active Disturbance Rejection Control for MEMS Gyroscopes. Transactions on Control systems Technology 2009; 17: 1432-1438.

[19] Momir R, etc. Optimized active disturbance rejection motion control with resonant extended state observer. ISSN 2019; 0020-7179: 1366-5820.

[20] Li J, Xia Y Q, Xiao H, Zhao P P. Robust absolute stability analysis for interval nonlinear active disturbance rejection based control system. ISA Transactions. Published by Elsevier Ltd. On behalf of ISA Journal homepage: www.elsevier.com/locate/isatrans 2017.

[21] Sun J L, Pu Z Q, Yi J Q. Conditional disturbance negation based active disturbance rejection Control for hypersonic vehicles. Control Engineering Practice 2019; 84: 156-171.

[22] Guo B Z, Wu Z H. Output tracking for a class of nonlinear systems with mismatched uncertainties by active disturbance rejection control. System & Control Letters 2017; 100: 21-31.

[23] Feng H Y P, Li S J. Active disturbance rejection control on weighted-moving-average-state-observer. J.Math.Anal App, 2014; 411: 354-361.

[24] Ren L N, Mao C H, Song Z Y, Liu F C. Study on active disturbance rejection

control with actuator saturation to reduce the load of a driving chain in wind turbines. Renewable Energy 2019; 133: 268-274.

[25] Ping D, Sebastien C, Patrick C. Disturbance rejection of battery/ultra capacitor hybrid energy sources. Control Engineering Practice, 2016; 54: 166-175.

[26] Castillo A, Garcia P, Sanz R, Albertos P. Enhanced extended state observer-based control for systems with mismatched uncertainties and disturbances. ISA Transactions. Journal homepage: www. elsevier. com/locate/isatrans 2017.

[27] Shi X X, Chen Y Q, Huang J C. Application of fractional-order active disturbance rejection controller on linear motion system. Control Engineering Practice 2019; 84: 156-171.

[28] Fu C F, Tan W. Control of unstable processes with time delays via ADRC. ISA Transactions. Journal homepage: www. elsevier. com/ locate/ isatrans 2017.

[29] Dong L L. Active Disturbance Rejection Control for an Electric Power Assist Steering System. International Journal of Intelligent Control and System 2010; 15: 18-24.

[30] She M, Fang X, Ohyama Y, Kobayashi H, Wu M. Improving disturbance rejection performance based on equivalent input disturbance approach. IEEE Trans. Ind. Electron 2008; 55: 380-389.

[31] Li S, Liu Z. Adaptive speed control for permanent-magnet-synchronous motor system with variations of load inertia. IEEE Trans Ind Electron 2009; 56: 3050-9.

[32] Xue W C, Huang Y. Performance analysis of active disturbance rejection tracking control for a class of uncertain LTI systems. ISA Transactions. Journal homepage: www. elsevier. com/ locate/ isatrans 2015.